Insights Into the Tectonic Stress History and Regional 4-D Natural Fracture Distribution in the Australian Cooper Basin Using Etchecopar's Calcite Twin Stress Inversion Technique, 2-D/3-D Seismic Interpretation and Natural Fracture Data From Image Logs and Core*

David Kulikowski[1], Khalid Amrouch[1], Khalda Hamed Mohammed Al Barwani[1], Wei Liu[1], and Dennis Cooke[1]

Search and Discovery Article #41752 (2015)
Posted December 21, 2015

*Adapted from extended abstract prepared in conjunction with oral presentation at AAPG/SEG International Conference & Exhibition, Melbourne, Australia, September 13-16, 2015, AAPG/SEG © 2015.

[1]Australian School of Petroleum, University of Adelaide, Adelaide, SA, Australia (david.kulikowski@adelaide.edu.au)

Abstract

A robust understanding of natural fractures can provide valuable information on subsurface fluid flow through optimally oriented fractures relative to the present day stress regime, and can be used as a tool to infer the stress orientation and regime of structural events that have affected a given area. The first part of the research utilises the fundamental principles of rock failure, combined with structural and stratigraphic seismic interpretation of two- and three-dimensional (2D and 3D) seismic data as well as pore pressure data, to investigate the potential relationship between fluid pressure and fracture/ fault distribution and density in Copper Basin. Secondly, and for the first time in Australia, the application of a new approach using the Etchecopar's calcite twin stress inversion technique (CSIT), along with rock mechanics and fault/fracture data, we will attempt to provide the complete stress tensors of individual structural events that affected the study area. These results will enhance the understanding of the complex structural history of the Cooper Basin, the largest onshore oil and gas province in Australia. Highly desirable information will be presented on the relationship between the timing of natural fracture development, complete natural fracture geometry, and structural event responsible for the development of the different fracture sets. In addition, the complete field scale fault geometry, timing of fault cessation, and geomechanical modelling of fault reactivation potential will be explored. This new approach that we apply to obtain a much more thorough understanding of the tectonic history of the region can also be beneficial in other complex basins around the world that have been affected by poly-phase structural events.

Study Area

The structurally complex Late Carboniferous to Middle Triassic intra-cratonic Cooper Basin is unconformably isolated from the underlying Cambrian to Carboniferous Warburton Basin, and overlying Jurassic to Cretaceous Eromanga Basin and spans an area of 130,000 km^2 across South Australia and Queensland (Figure 1 and Figure 2) (Kantsler et al., 1984; Bradshaw, 1993; Apak, 1997; Gravestock and Jensen-Schmidt, 1998; Mavromatidis, 2006; Reynolds et al., 2006). Initial accommodation space and NE-SW and SE-NW striking lineaments are believed to have developed during the Neo-Proterozoic SE-NW oriented extensional period (Apak et al., 1997; Haines et al., 2001; Muller et al., 2012).

Subsequent structural movement during the Silurian to Carboniferous, Sakmarian, late Permian, Upper Triassic, and Upper Cretaceous reactivated these pre-existing structural features to give the present day structural architecture (Apak et al., 1997; Mavromatidis, 2006). The NE-SW striking Gidgealpa-Merrimelia-Innamincka (GMI) and Murteree-Nappacoongee (MN) Ridges structurally isolate the Patchawarra, Nappamerri and Tenappera Troughs (Figure 2).

The South Australian portion of the basin contains the thickest of low permeability hydrocarbon bearing formations, and hence the greatest density of well data and seismic surveys. Glacial deposition of the Merrimelia Formation commenced in the early Permian and marks the base of the Cooper Basin, with the fluvial Tirrawarra Formation deposited soon after (Figure 1) (Kantsler et al., 1984; Apak et al., 1997). The middle Permian Patchawarra Formation contains cyclically deposited coals, shales and sands, and is the major hydrocarbon source (Figure 1) (Boreham and Hill, 2011). Subsequent depositional environments transition from lacustrine deltas to shoreline, deltaic, fluvial, and lacustrine prior to large-scale structural movements in the Upper Triassic (Figure 1) (Kantsler et al., 1984; Bradshaw, 1993; Apak et al., 1997; Boreham and Hill, 2011). The major producing zones are low permeability and require fracture stimulation treatments to be economically lucrative; therefore, a complete understanding of natural fracture geometry and timing of natural fracture development would benefit exploration and production companies currently operating in the region. An improved understanding of true fault geometry, timing of fault cessation, and the reactivation potential of faults under the present day stress regime is beneficial in better understanding hydrocarbon migration.

Methodology

Natural fracture and bedding plane data was obtained from 27 borehole image logs from the South Australian portion of the Cooper Basin (Figure 2). This portion of the basin is completely overlain with loose sediment rendering it impossible to directly measure fracture data from outcrop. Our interpreted natural fracture data was collated to stratigraphy and individual wells using Win-tensor (Delvaux, 1993; Delvaux and Spencer, 2003) to allow a detailed analysis of natural fracture density and geometry with time and space. We aim to identify natural fractures in core to analyse, the mode of opening as well as cross cutting relationships. The analysis of fracture sets follows a straightforward methodology, aligning with the fundamental rock failure principals, to infer a paleo-stress orientation and stress regime (Anderson, 1951; Zoback et al, 1989; Zoback et al., 2003). Upon completing this component of the research, our efforts will shift to constraining the magnitude and orientation of structural events within the Cooper Basin through the combination of fracture data with the Etchecopar's calcite twin stress inversion technique (CSIT).

Etchecopar's CSIT (Etchecopar, 1984) leads directly to the simultaneous computation of principal stress orientations (with: $\sigma1$- maximum principal stress; $\sigma2$- intermediate principal stress; $\sigma3$- minimum principal stress) and differential stresses (Tourneret and Laurent, 1990; Lacombe and Laurent, 1996; Amrouch et al., 2010a), which also yields data on the ellipsoid shape ratio $\Phi=(\sigma2-\sigma3)/(\sigma1-\sigma3)$, and the peak differential stress ($\sigma1-\sigma3$) (with $\sigma1\geq\sigma2\geq\sigma3$ as a compressive stresses, positive in value). The tensor solution is calculated as a normalised reduced stress tensor, such that ($\sigma1-\sigma3$), and is scaled to [($\sigma1-\sigma3$)*=1] (Arboit et al., 2015). Core samples containing calcite are converted into thin section (Figure 3A) and analysed under a universal stage microscope (Figure 3B) to measure the dip angle and strike of twinned planes within individual calcite crystals (Figure 3C). Calcite twinning is a deformation mechanism responding to simple shear that is applied to part of the host crystal with twinned planes developing in a known geometry given the resolved shear stress exceeds 10 MPa (Figure 3D) (Lacombe and Laurent, 1996).

Following on from these methods, we will attempt to better understand the periods of fault reactivation that may have jeopardised hydrocarbon preservation and potentially altered migration pathways through time by attempting to find a relationship between the orientation of structural events with the interpreted true fault geometry and timing of fault cessation. Structural and stratigraphic interpretation of seven 3D seismic surveys will be integrated with previous research in an attempt to associate individual structural events with the fault geometry preferentially created/ reactivated at a particular time. Each of these seismic surveys were depth converted using a velocity model that we generated using well check-shots and formation top data. This enabled us to accurately interpret the seismic data in the depth domain, which shows true geometries and thicknesses. Two selected surveys will be geomechanically modelled to predict the reactivation potential (slip tendency, dilation tendency, and fracture stability) of faults under the present day stress regime. Future work will apply a similar methodology to the Queensland portion of the Cooper Basin.

In order to accurately geomechanically model the potential reactivation of faults, an understanding of reservoir pressure is required. Rather than conduct a local pore pressure and temperate analysis on a small number of fields, we will conduct a regional analysis of pore pressure across the South Australian portion of the basin. Available pressure and temperature data will be collated from each well to compare reservoir pressures and temperatures spatially across the basin, as well as with depth. Ultimately, pore pressure, temperature, natural fracture density, and fault density maps will be overlapped in an attempt to find a correlation.

Results and Interpretations

Fracture sets:

From the 27 borehole image logs, we interpreted 668 natural fracture planes and their associated bedding planes (Figure 4). Three dominant natural fracture strike directions (N-S, NE-SW, and SE-NW) are interpreted (Figure 4A), all of the interpreted bedding planes showing an average strike of approximately E-W (Figure 4C). It is important to note, however, that the dip angle of natural fractures varies from near horizontal to near vertical, with bedding planes between horizontal and approximately 70 degrees (Figure 4). Natural fracture data is displayed per well to show the variation in geometry and density across the basin. From a high-level view, it appears that fracture density is greatest in wells along structural highs, and lowest within the three main troughs (Kulikowski et al., 2015a). Natural fracture data from Figure 4 were reorganised into five conjugated natural fracture sets and one mode 1 opening set modelled to infer a likely paleo-stress orientation for their development (Figure 5). Two conjugated natural fracture sets (FS_5 and FS_6) appear throughout the entire stratigraphic column and are modelled to have occurred under an extensional stress regime in a NE-SW and SE-NW direction (Figure 5).

Seismic data:

Seven 3D seismic surveys were chosen for structural and stratigraphic interpretation based on the timing of acquisition, large volume of well control, and proximity to the major NE-SW striking GMI and MN Ridges (Figure 6-1). The strike, pole to fault plane, and stereographic projection of each interpreted fault is shown in Figure 6-2. The cumulative strike of each fault shows a dominant NE-SW strike, with N-S, E-W and SE-NW striking faults also present (Figure 6-2v). It is evident that a majority of faults have a high dip angle of approximately 60 degrees from horizontal. A small sample size of near vertical SE-NW striking faults appears within each of the 3D seismic volumes. Grant-Woolley et

al. (2014) also identified a number of near vertical SE-NW striking strike-slips faults within the Cooper Basin, and suggested that these particular faults may pose tremendous implications on reservoir compartmentalisation and a decrease in reservoir quality because of cataclasis. Our study aims to constrain the timing of fault cessation and attempts to find a relationship between fault geometries that are preferentially reactivated through time with individual structural events.

Fracture and fault data will also be integrated with pore pressure and temperature data across the entire South Australian portion of the Cooper Basin to assess the existence of a potential relationship. Pore pressure and temperature maps will be generated across the study area for various stratal packages. Drill-stem test (DST), formation multi-test (FMT), and repeat formation test (RFT) data will form the framework for this analysis. From an initial investigation, we expect to have over 6000 pore pressure data points from a large variety of stratal units.

Discussion

Our natural fracture interpretation of borehole image logs across the Australian Cooper Basin provides complete data to discuss the relative timing (pre-, syn-, post-folding) of natural fracture development and the geometry of regionally systematic natural fracture networks. Results show three dominant natural fracture strike directions (N-S, NE-SW, and SE-NW) and a dominant NE-SW striking fault system with approximately 60 degrees of dip from horizontal. Our measured natural fractures, together with literature, infers that the N-S Alice Springs Orogeny, SE-NW Sakmarian compression, E-W Triassic (Hunter-Bowen Orogeny) and Cretaceous compression, and N-S Paleogene compression contributed to the development of natural fractures, and thus to the structural evolution of the basin (Kulikowski et al., 2015a). The alignment of NE-SW and SE-NW striking high angle natural fractures closely resembles the major basement involved structural lineaments throughout the basin. Stress inversion modelling of these particular natural fractures infers that an extensional regime was present during basin development. It is likely that post compressional flexural relaxation, or sag, focused along pre-existing structural lineaments is responsible for their development. These natural fractures are also optimally oriented for reactivation under the present day stress regime, and most likely to be open to fluid flow. It is these natural fracture geometries that would most likely improve the economic feasibility of low permeability hydrocarbon reservoirs that are prolific in the Cooper Basin.

Our research into constraining the timing of fault cessation and measuring the true field scale fault geometry enabled us to conclude; [1] the dominant field scale fault geometry is high angle with a NE-SW strike; [2] SE-NW striking vertical faults either developed under a strike-slip stress regime during the N-S Carboniferous Alice Springs Orogeny, or pre-existing SE-NW striking vertical faults were reactivated by this N-S directed stress to give a dextral sense of motion; [3] NE-SW striking high angle faults were active during the SE-NW Sakmarian compressional event; [4] SE-NW striking high angle faults were active during the crustal shortening associated with the NE-SW oriented Daralingie unconformity event; [5] N-S striking high angle faults and the main NE-SW striking GMI and MN Ridges were active during the E-W Hunter-Bowen Orogeny; [6] the final stage of fault movement was interpreted during the E-W Late Cretaceous crustal shortening event (Kulikowski et al., 2015b). A similar approach will be applied to the Queensland portion of the basin, with the addition of geomechanical modelling to predict the reactivation potential of faults under the present day stress.

Future work should investigate the effect of field scale SE-NW strike-slip faults within each of the seven 3D seismic volumes. The complete stress tensor of individual structural events will be constrained and integrated with fracture and fault interpretations to define the likely timing

of development and reactivation. An insight into the pore pressure and temperature variation across the basin will examine the possible relationships with fracture and fault data. The application of this methodology to other complex basins across the world will enhance the understanding of the micro-, meso-, and macro-scale deformation exhibited throughout basin development.

Conclusion

Our research into the structural and stress history of the Australian Cooper Basin has yielded valuable information on natural fracture geometry and the timing of natural fracture development, which we used to infer the most likely stress orientation and regime through time. The 4D analysis that we employed to interpret fracture sets from well log data is commonly overlooked and mostly only the strike direction of natural fractures is analysed, overlooking the complete geometry of the fractures and their relationship with bedding. The final stage of our research helped to reduce the uncertainty associated with paleo-stress orientations and magnitudes by applying Etchecopar's CSIT for the first time in an Australian basin. This research highlights the potential of this approach by improving the understanding of paleo-stress within one of the most complex basins in Australia and may lead to similar studies being applied to other Australian basins.

Acknowledgements

The authors would like to acknowledge the financial contribution made by the GeoFrac Consortium, which includes the sponsoring companies; Santos, Beach Energy, Chevron, Halliburton and GB Group (QGC). Many thanks to DUG Insight, Paradigm, Schlumberger, JRS, and the designer of Win-tensor for their generous donation of academic licenses.

References Cited

Alexander, E.M., D.I. Gravestock, C. Cubitt, and A. Chaney, 2011, Lithostratigraphy and Environments of Deposition: Petroleum Geology of South Australia, Cooper Basin, v. 4, Ch. 6, Primary Industries and Resources.

Amrouch, K., O. Lacombe, N. Bellahsen, J.M. Daniel, and J.P. Callot, 2010a, Stress and strain patterns, kinematics and deformation mechanisms in a basement‐cored anticline: Sheep Mountain Anticline, Wyoming: Tectonics, v. 29/1, TC1005, doi:10.1029/2009TC002525.

Anderson, E.M., 1951, The Dynamics of Faulting and Dyke Formation With Application to Britain: Hafner Pub. Co., Oliver and Boyd, London.

Apak, S.N., W.J. Stuart, N.M. Lemon, and G. Wood, 1997, Structural evolution of the Permian-Triassic Cooper Basin, Australia: relation to hydrocarbon trap styles: AAPG Bulletin, v. 81/4, p. 533-555.

Arboit, F., K. Amrouch, A.S. Collins, R. King, and C. Morley, 2015, Determination of the tectonic evolution from faults and calcite twins on the western margin of the Indochina Block: Tectonics, In Press.

Backé, G., H. Abul Khair, R. King, and S. Holford, 2011, Fracture mapping and modelling in shale-gas target in the Cooper basin, South Australia: APPEA Journal, v. 51, p. 397-410.

Boreham, C.J., and A.J. Hill, 2011, Source Rock Distribution and Geochemistry: Petroleum Geology of South Australia, Cooper Basin, v. 4, Ch. 8, Primary Industries and Resources.

Bradshaw, M.T., 1993, Australian petroleum systems: PESA Journal, v. 21, p. 43-53.

Delvaux, D., 1993, The TENSOR program for paleostress reconstruction: examples from the east African and the Baikal rift zones: EUG VII Strasbourg, France, 4-8 April 1993. Abstract supplement N°1 to Terra Nova, v. 5, p. 216.

Delvaux, D., and B. Sperner, 2003, Stress tensor inversion from fault kinematic indicators and focal mechanism data: the TENSOR program: in New Insights into Structural Interpretation and Modelling, D. Nieuwland, ed., Geological Society, London, Special Publications, v. 212: p. 75-100.

Etchecopar, A., 1984, Etude des e tats de contraintes en tectonique cassante et simulationc de de formation plastique (approche mathe matique): the se doctorates-sciences, 270 pp., Univ. Sci. et Tech. du Langue-doc, Montpellier, France.

Gatehouse, C.G., 1986, The geology of the Warburton Basin in South Australia: Australian Journal of Earth Sciences, v. 33/2, p. 161-180.

Grant-Woolley, L., A. Kong, B. Schoemaker, H. Nasreddin, and E.T. Montague, 2014, Identification of Strike-Slip Faults Provides Insights into the Further Development of Mature Cooper Basin Fields: in SPE Asia Pacific Oil & Gas Conference and Exhibition, Society of Petroleum Engineers.

Gravestock, D.I., and B. Jensen-Schmidt, 1998, Structural setting: Petroleum Geology of South Australia, v. 4, p. 47-67.

Haines, P.W., M. Hand, and M. Sandiford, 2001, Palaeozoic synorogenic sedimentation in central and northern Australia: a review of distribution and timing with implications for the evolution of intracontinental orogens: Australian Journal of Earth Sciences, v. 48/6, p. 911-928.

Kantsler, A.J., T.J.C. Prudence, A.C. Cook, and M. Zwigulis, 1983, Hydrocarbon habitat of the Cooper/Eromanga basin, Australia: Australian Petroleum Exploration Association Journal, v. 23/1, p. 75-92.

Khair, H.A., D. Cooke, and M. Hand, 2013, The effect of present day in situ stresses and paleo-stresses on locating sweet spots in unconventional reservoirs, a case study from Moomba-Big Lake fields, Cooper Basin, South Australia: Journal of Petroleum Exploration and Production Technology, v. 3/4, p. 207-221.

Kuang, K.S., 1985, History and style of Cooper–Eromanga Basin structures: Exploration Geophysics, v. 16/2-3, p. 245-248.

Kulikowski, D., K. Amrouch, and D. Cooke, 2015a, Insights into the structural history in the Cooper Basin, Tectonics, submitted.

Kulikowski, D., K. Amrouch, and D. Cooke, 2015b, Constraining the regional fault geometry and timing of fault cessation in the Australian Cooper Basin, Interpretation, submitted.

Lacombe, O., and P. Laurent, 1996, Determination of deviatoric stress tensors based on inversion of calcite twin data from experimentally deformed monophase samples: preliminary results: Tectonophysics, v. 255/3, p. 189-202.

Lowe-Young, B.S., S.I. Mackie, and R.S. Heath, 1997, The Cooper-Eromanga Petroleum System, Australia: Investigation of Essential Elements and Processes.

Mavromatidis, A., 2006, Burial/exhumation histories for the Cooper–Eromanga Basins and implications for hydrocarbon exploration, Eastern Australia: Basin Research, v. 18/3, p. 351-373.

Müller, R.D., and S. Dyksterhuis, 2012, Current and palaeo-stress models for central Australian basins: in Proceedings of the Central Australian Basins Symposium, Alice Springs, August, 2005 ed. by Munson, T.J. and Ambrose, G.J., Northern Territory Geological Survey Special Publication 2, p. 1-9.

Powell, C.M.A., 1984, Uluru and Adelaidean regimes; Late Devonian and Early Carboniferous: in J.J. Veevers, ed., Phanerozoic earth history of Australia: Oxford, Clarendon Press, p. 329-339.

Reynolds, S.D., S.D. Mildren, R.R. Hillis, and J.J. Meyer, 2006, Constraining stress magnitudes using petroleum exploration data in the Cooper–Eromanga Basins, Australia: Tectonophysics, v. 415/1, p. 123-140.

Rezaee, M.R., and X. Sun, 2007, Fracture‐Filling Cements in the Palaeozoic Warburton Basin, South Australia: Journal of Petroleum Geology, v. 30/1, p. 79-90.

Tourneret, C., and P. Laurent, 1990, Paleostress orientations from calcite twins in the North Pyrenean foreland by the Etchecopar inverse method: Tectonophysics, v. 180, p. 287-302.

Turner, F.J., and M. Orozco, 1976, Crystal bending in metamorphic calcite, and its relations to associated twinning: Contributions to Mineralogy and Petrology, v. 57/1, p. 83-97.

South Australian Resources Information Geoserver (SARIG), Depth to basement map. Web Accessed November 25, 2015, https://sarig.pir.sa.gov.au/Map.

Sun, X., 1997, Structural style of the Warburton Basin and control in the Cooper and Eromanga Basins, South Australia: Exploration Geophysics, v. 28/3, p. 333-339.

Zoback, M.L., M.D. Zoback, J. Adams, M. Assumpcao, S. Bell, E.A. Bergman, and M. Zhizhin, 1989, Global patterns of tectonic stress: Nature, v. 341, p. 291-298.

Zoback, M.D., C.A. Barton, M. Brudy, D.A. Castillo, T. Finkbeiner, B.R. Grollimund, and D.J. Wiprut, 2003, Determination of stress orientation and magnitude in deep wells: International Journal of Rock Mechanics and Mining Sciences, v. 40/7, p. 1049-1076.

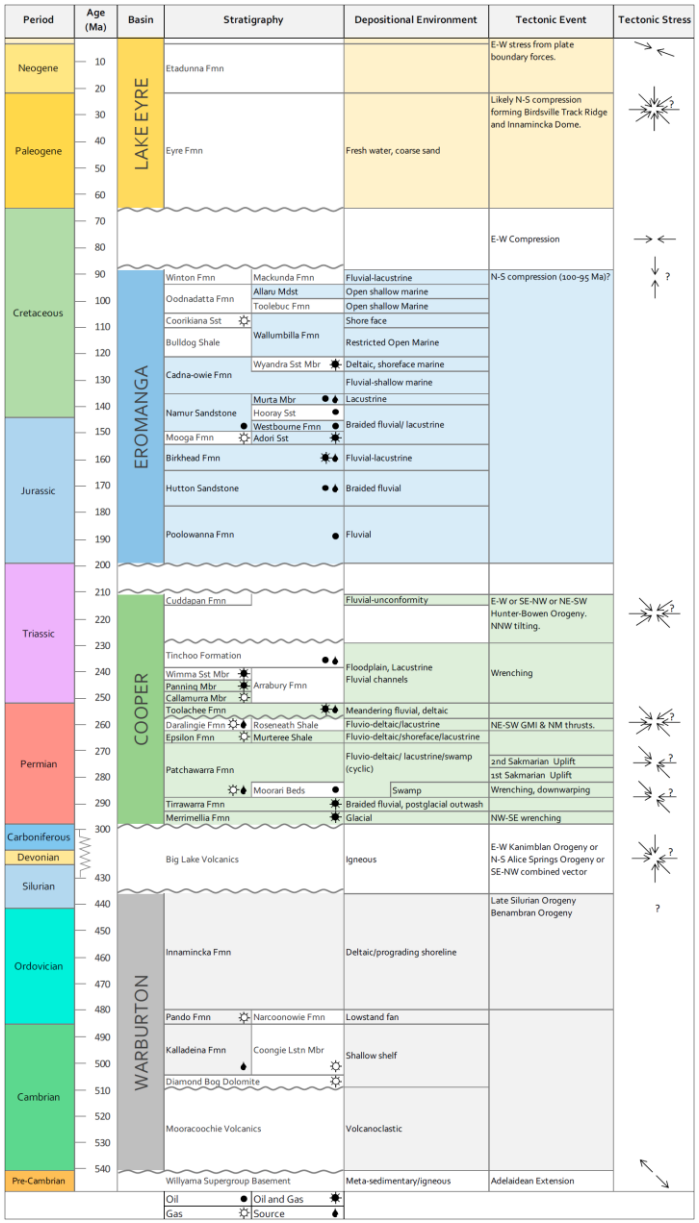

Figure 1. Summary of the Warburton, Cooper, Eromanga and Lake Eyre Basin. Highlighted stratigraphic units are used in this research (Kantsler et al., 1984; Powell, 1984; Kuang, 1985; Gatehouse, 1986; Apak et al., 1997; Lowe-Young et al., 1997; Sun, 1997; Haines et al., 2001; Mavromatidis, 2006; Rezaee and Sun, 2007; Backe et al., 2010; Alexander et al., 2011; Muller et al., 2012; Khair et al, 2013; modified from Kulikowski et al., 2015a).

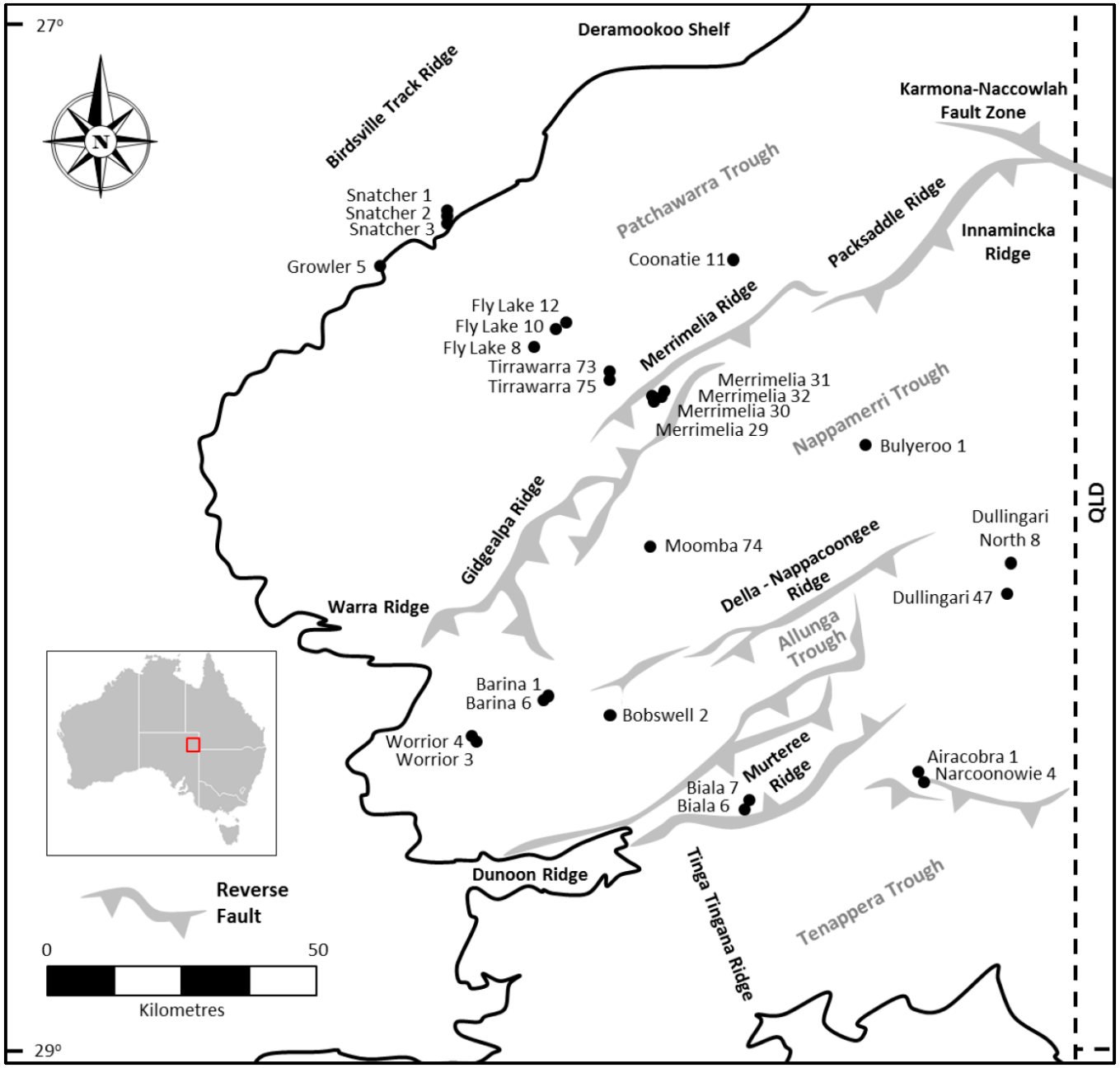

Figure 2. Structural map of the Cooper Basin overlain by wells that contain borehole image logs (modified from Kulikowski et al., 2015a; modified after Rezaee and Sun, 2007).

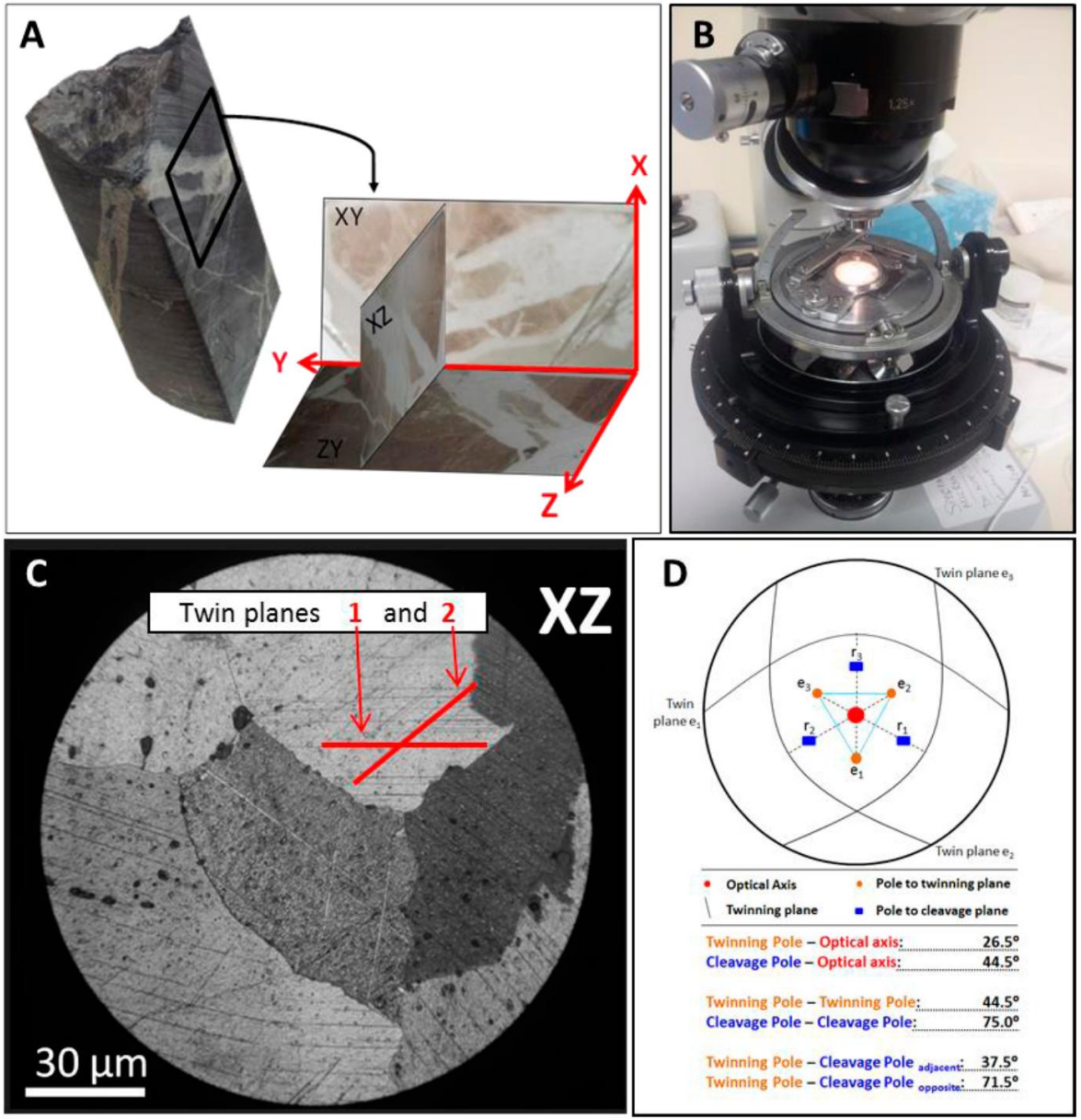

Figure 3. [A] Sampling procedure from core to thin section - example from Gidgealpa 5; [B] The universal stage microscope available at the Australian School of Petroleum capable of measuring orientation and dip; [C] Calcite crystals through a universal stage microscope - example from the Gidgealpa 5 Kalladeina Formation showing at least two twin planes in a given crystal; and [D] The structural configuration of a calcite crystal (modified from Kulikowski et al., 2015a; after Turner and Orozco, 1976).

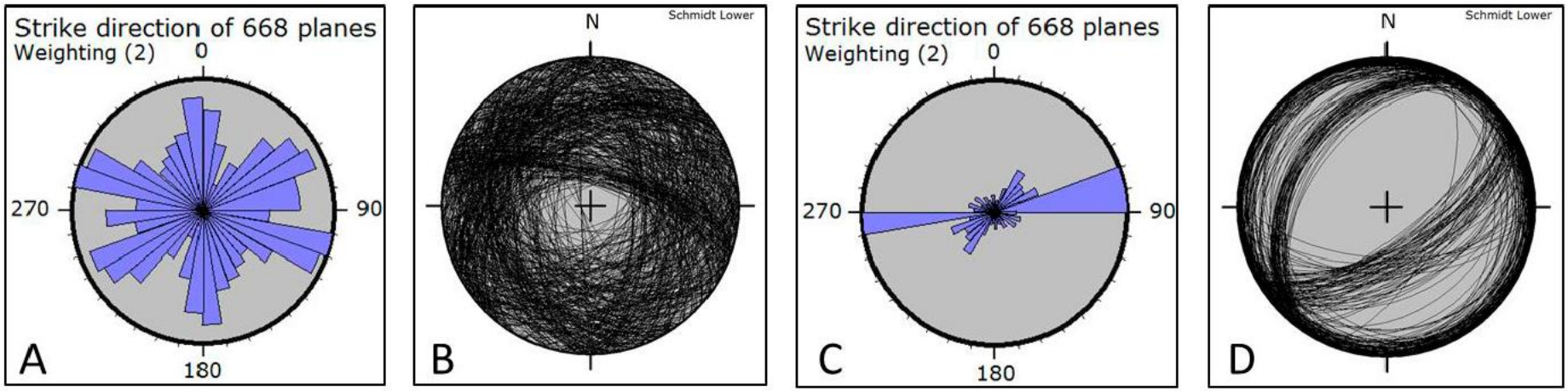

Figure 4. [A] Cumulative fracture plane strike; [B] Cumulative fracture plane stereographic projection; [C] Cumulative bedding plane strike; and [D] Cumulative bedding plane stereographic projection (modified from Kulikowski et al., 2015a).

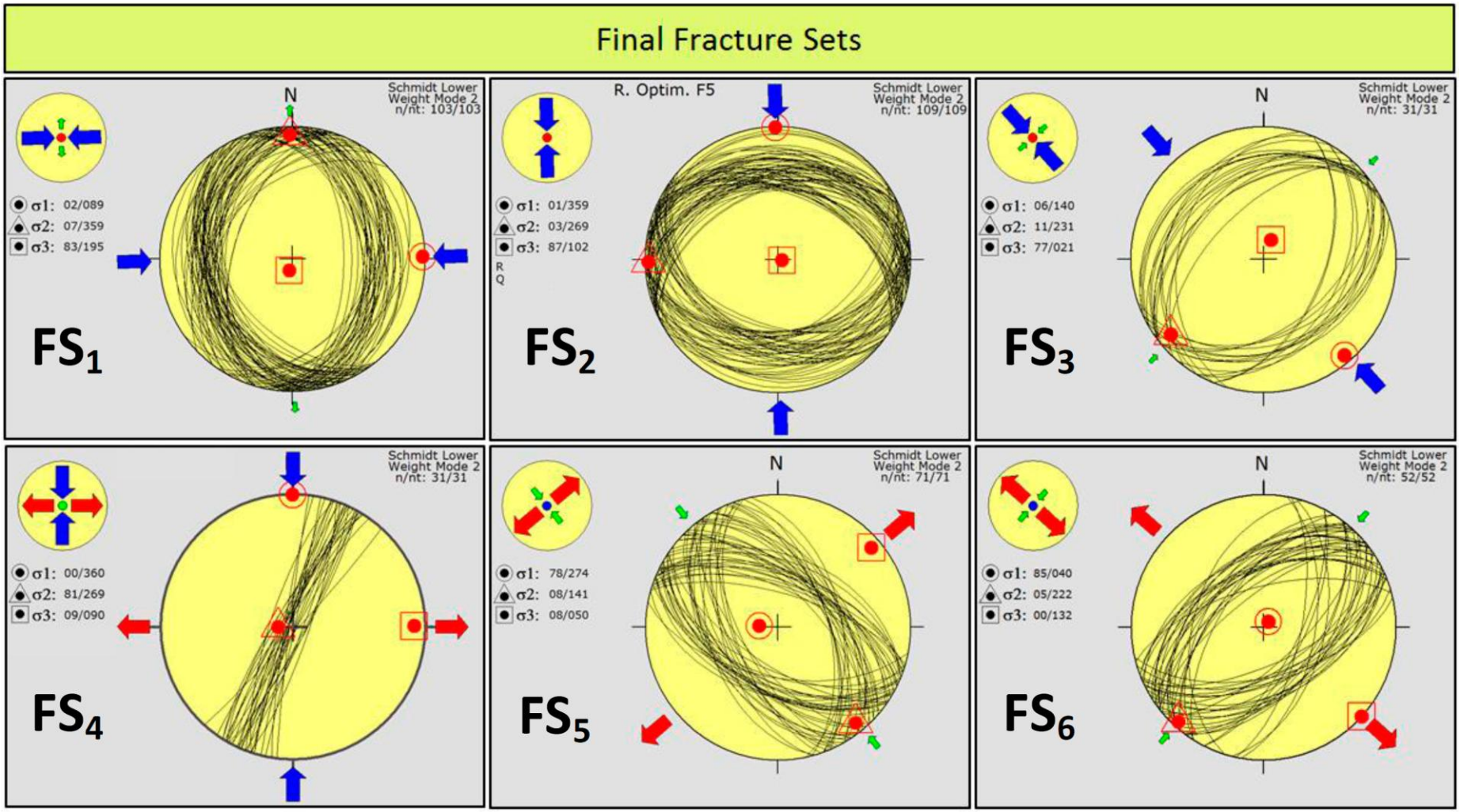

Figure 5. Fracture data used in this study separated into 6 fracture sets across all formations. FS5 and FS6 occur throughout the sedimentary column (modified from Kulikowski et al., 2015b).

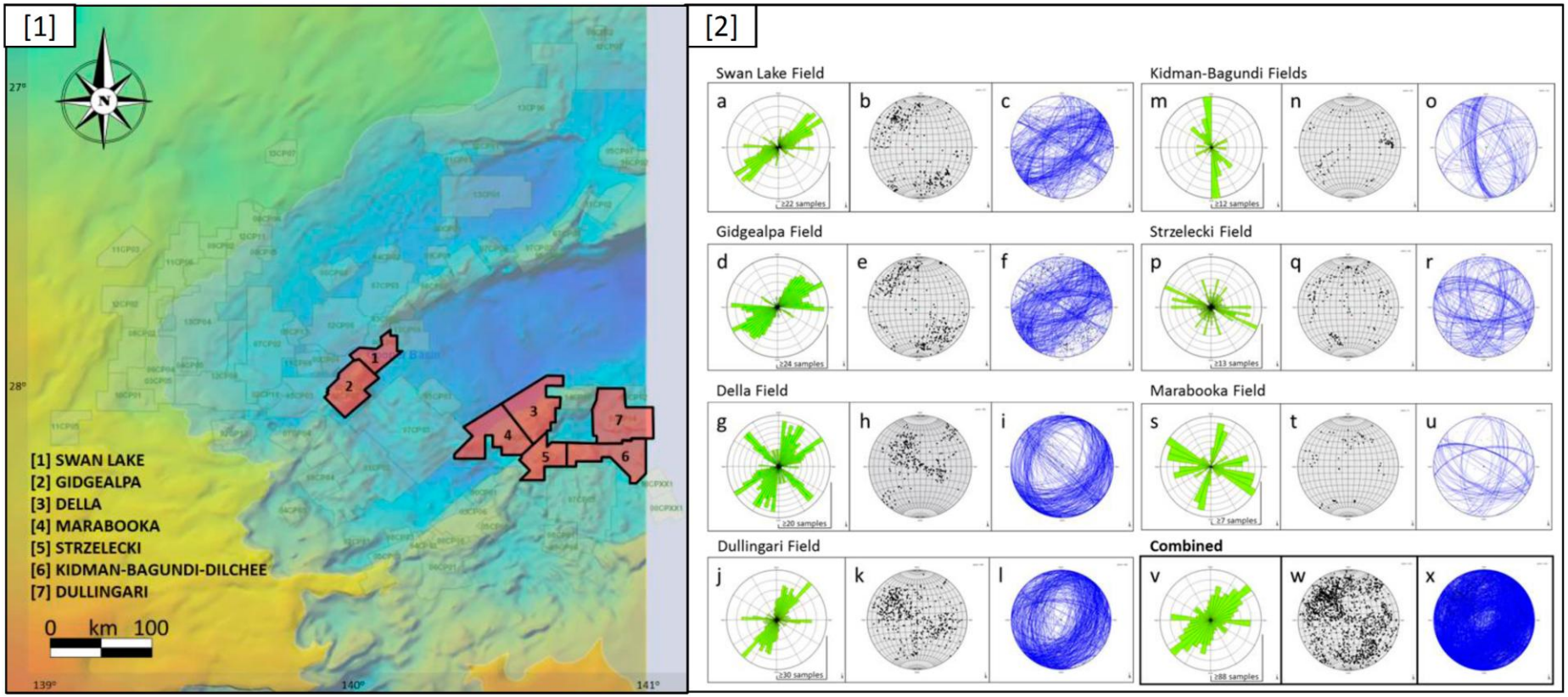

Figure 6. [1] Location of the 3D seismic surveys used for this study (modified after SARIG, 2015); [2] Complete basement fault geometry from each of the interpreted 3D seismic surveys. Strike, poles to planes, and stereographic projection of all faults is shown. A sample density of 20 was used for each fault (modified from Kulikowski et al., 2015b).